Absence of quantum anomalous Hall state in 4*d* transition-metal-doped Bi_2Se_3: An *ab initio* study

Bei Deng,[1,3] Feng Liu,[2] and Junyi Zhu[1,*]

[1]*Department of Physics, the Chinese University of Hong Kong, Hong Kong, China*

[2]*Department of Materials Science and Engineering, University of Utah, Salt Lake City, Utah 84112, USA*

[3]*Department of Physics, Southern University of Science and Technology, Shenzhen 518055, China*

(Received 20 June 2017; published 6 November 2017)

The realization of insulating ferromagnetic states in topological insulator (TI) systems, with sufficiently high Curie temperatures (T_C) and large magnetically induced gaps, has been the key bottleneck towards the realization of the quantum anomalous Hall effect (QAHE). Despite the limited reports on 3*d* or 4*f* transition-metal (TM)-doped Bi_2Se_3, there remains a lack of systematic studies on 4*d* TMs, which may be potential candidates since the atomic sizes of 4*d* TMs and that of Bi are similar. Here, we report a theoretical work that probes the magnetic behaviors of the 4*d* TM-doped Bi_2Se_3 system. We discovered that among the 4*d* TMs, Nb and Mo can create magnetic moments of 1.76 and 2.96 μB in Bi_2Se_3, respectively. While Mo yields a stable gapless antiferromagnetic ground state, Nb favors a strong ferromagnetic order, with the magnetic coupling strength (T_C) ~6 times of that induced by the traditional Cr impurity. Yet, we found that Nb is still unfavorable to support the QAH state in Bi_2Se_3 because of the reduced correlation in the t_{2g} band that gives a gapless character. This rationale is not only successful in interpreting why Nb, the strongest candidate among 4*d* TMs for achieving ferromagnetism in Bi_2Se_3, actually cannot lead to QAHE in the Bi_2Se_3 system even with the assistance of codoping but also is particularly important to fully understand the mechanism of acquisition of insulating ferromagnetic states inside TI. On the other hand, we discovered that Mo-doped Bi_2Se_3 favors strong antiferromagnetic states and may lead to superconducting states.

DOI: 10.1103/PhysRevB.96.174404

I. INTRODUCTION

Discovered in magnetic topological insulator (TI) systems, the quantum anomalous Hall effect (QAHE) has recently attracted a growing interest since its experimental realization [1–8], both fundamentally and for practical applications of spintronic devices. The dissipationless chiral edge states in the QAH insulator could potentially lead to applications such as interconnects of integrated circuits and spintronics [9,10]. Although numerous models have been proposed to realize this effect at higher temperatures [11–14] to facilitate its realistic applications, the crucial temperatures, thus far from its experimental observations, have been restricted to be below 2 K [8].

The QAHE originates from the spin-orbit coupling (SOC), combined with time reversal symmetry breaking perturbations such as long-range ferromagnetic (FM) ordering, giving rise to the quantized Hall conductance with the absence of an external magnetic field [10,15]. The major challenges for high-temperature QAHE mainly comes from the low FM Curie temperature, together with the extremely small gaps in magnetically doped TI: (i) The former, as previously reported [8,16,17], is usually attributed to the limited doping efficiency/solubility of the magnetic impurities and the insufficient couplings between them. In particular, the magnetic impurity Cr, the first element that leads to the QAHE in $(Bi_xSb_{1-x})_2Te_3$ system, is actually observed to favor a short range distribution in the TI thin film because of its small atomic radius, severely hindering its realistic doping efficiency for a long-range magnetic order. Furthermore, the magnetic coupling strength between these impurities is only in the order of 10 meV [18] so that the T_C for such magnetic TI system is usually rather low. (ii) The latter basically originates from the fundamental fact that the SOC in the 3*d* transition-metal (TM)-doped system is not so strong and also that some of these impurities may form defect states that may further reduce the band gap.

Apart from these 3*d* TMs, intuitively the 4*d* TM may be better candidates for long-range magnetic orders in TI and thereby for the realization of QAHE, which can be understood in the following way. (1) First, the atomic radii of these 4*d* TMs are much more comparable to that of the Bi atoms in the host system, leading to smaller lattice distortions, which can be beneficial in improving the doping efficiency. (2) The atomic masses of these 4*d* TMs are larger than those of the 3*d* TMs so that the SOC can be enhanced, which could further benefit the magnetically induced band gap due to the Van Vleck mechanism [19]. (3) In a similar regard, the magnetic coupling strength between these 4*d* impurities may also be stronger, owing to the enhanced Van Vleck spin susceptibility, consequently leading to a higher T_C. These considerations have motivated us to explore the 4*d* TM impurities doped TI systems for the realization of QAHE at high temperatures.

We have investigated the 4*d* TM-doped Bi_2Se_3 system as a prototypical example, using the *ab initio* calculations based on density functional theory. We have found that among all the 4*d* TM impurities, the substitutions of the Nb atoms on the Bi sites can lead to a substantially stronger FM order, associated with those of the Cr atoms, suggesting a higher Curie temperature. Furthermore, we have shown that a compressive biaxial stress, which can be achieved straightforwardly by employing epitaxial strains, can improve the solubility of the Nb impurity and its magnetic moment as well. However, Nb is still unfavorable in supporting the insulating FM and QAH states in Bi_2Se_3 due to the reduced correlation effect in t_{2g} bands rising from the strong *p*-*d* hybridization between the t_{2g} triplet and the *p* states of Se, which dilutes the electron correlation and in turn gives rise

*jyzhu@cuhk.edu.hk

to a gapless character. This rationale is found to be general to interpret why such TMs cannot lead to QAHE in such systems. In addition, we show that the substitution of Mo on the Bi sites leads to a moderately strong antiferromagnetic (AFM) ordering, which may potentially support a topological superconducting phase.

II. COMPUTATIONAL METHOD AND DETAILS

For this paper, we used the Vienna *Ab initio* Simulation Package (VASP) code [20], with spin polarized generalized gradient approximation (GGA) and Perdew-Burke-Ernzerhof (PBE) functional for exchange-correlation [21]. Projector augmented wave (PAW) pseudopotentials [22] for Bi, Se, and 4*d* TMs were used with a plane wave basis-set cutoff energy of 350 eV, while 4*s* semicore electrons were also treated as the valency in the calculation. The SOC was included in all the calculations, except as mentioned otherwise. The geometry of isolated impurities was modeled by using a 60-atom supercell, consisting of $2 \times 2 \times 1$ conventional Bi_2Se_3 cells in the hexagonal lattice. A Γ-centered $7 \times 7 \times 2$ Monkhorst-Pack mesh was used for k-point sampling in the Brillouin zone. In the geometry optimization, all the atoms were allowed to relax until the calculated Hellmann-Feynman forces are less than 5 meV/Å.

We calculated the formation energy of TM impurities and investigated the spin-polarized electronic structure of these impurities in Bi_2Se_3. We chose Bi_2Se_3 as the objective host system, mainly because of its high similarity with the $(Bi_xSb_{1-x})_2Te_3$ in electronic and geometric structures and because many theoretical models [18,19] predicated on Bi_2Se_3-system-based QAHE have been successfully realized in $(Bi_xSb_{1-x})_2Te_3$ systems [1,2]. The defect formation energy is defined as [23]

$$\Delta H_f(\mathrm{TM}) = E_{\mathrm{tot}}(\mathrm{Bi_2Se_3 : TM}) - E_{\mathrm{tot}}(\mathrm{host}) - \sum\nolimits_i n_i \mu_i, \quad (1)$$

where E_{tot} (Bi_2Se_3:TM) is the total energy of a supercell with one charge neutral impurity; E_{tot} (host) is the total energy of the supercell with the absence of impurity; n_i is the number of certain impurity atoms added to ($n_i < 0$) or removed from ($n_i > 0$) the supercell; and μ_i is the corresponding chemical potential. The *chemical potentials* should fulfill the following conditions: (i) $2\mu_{\mathrm{Bi}} + 3\mu_{\mathrm{Se}} = \Delta H_f$ (Bi_2Se_3) to keep the host material thermodynamically stable; (ii) $x\ \mu_{\mathrm{TM}} + y\ \mu_{\mathrm{Se}} \leqslant \Delta H_f$ (TM_xSe_y) to avoid formations of secondary phases of TM_xSe_y; and (iii) $\mu_i < 0$ to avoid precipitations of elementary substances for both host and TM elements.

III. RESULTS AND DISCUSSIONS

First, we have considered the magnetic moment for all the 4*d* TMs. From several previous studies [13,18,24], we conclude that the 3*d* TM impurity normally favors the substitution Bi site in Bi_2Se_3 with respect to the substitution Se sites or interstitial sites. This would suggest that the 4*d* TMs will favor the cation Bi site even more because their atomic radii are more comparable to the host Bi atom. Therefore, here we report only the magnetic moments for the 4*d* TMs occupying the Bi sites. The calculated magnetic moments, when significant, are shown in Table I. One notices that among the 4*d* TMs, Mo can create a magnetic moment of 2.96 μB, comparable to the magnetic moment of 3*d* TM Cr. However, the Mo impurity may not be as promising as Cr in realizing QAHE. This is because, although Mo_{Bi} has a moderately large magnetic moment in Bi_2Se_3, the magnetic moments favor the coupling in the antiparallel direction, leading to a strong AFM ground state, which negates the creation of QAHE that requires a FM ground state. On the other hand, the resulting antiferromagnetism, from Mo doping, may potentially lead to a topological superconducting phase supported by the Cooper pairing model, which can be mediated by the strong AFM spin fluctuations, as proposed in a few theoretical studies [25–27].

TABLE I. Calculated magnetic moment of Zr_{Bi}, Nb_{Bi}, Mo_{Bi}, Ru_{Bi}, and Rh_{Bi} in Bi_2Se_3; the magnetic coupling strength ($\Delta E_{\mathrm{FM-AFM}}/2$) is given here for Nb_{Bi} and Mo_{Bi}.

Dopant	Zr_{Bi}	Nb_{Bi}	Mo_{Bi}	Ru_{Bi}	Rh_{Bi}
$\Delta E_{\mathrm{FM-AFM}}/2$ (meV)	–	– 69.5	32	–	–
Magnetic moment (μB)	0	1.76	2.96	1.00	0

In this paper, the magnetic coupling strength ($\Delta E_{\mathrm{FM-AFM}}/2$) of a given species of impurity is defined here as a half of the energy difference between the FM configuration and its AFM counterpart, which is calculated by placing two magnetic atoms in the supercell geometry of Bi_2Se_3 with a variation of distances where the FM state corresponds to a configuration in which the two atoms have a parallel spin and the AFM state corresponds to a configuration having the two atoms with antiparallel spin. For layered materials such as Bi_2Se_3, the FM/AFM coupling strengths would depend not only on the impurity distance/concentration, but also on their spin patterns. For instance, the Mo impurity favors an A-type-like AFM configuration, where two atoms of antiparallel spins are in different atomic layers (here only the second and third neighbors are subject to such a configuration), while the C-type-like configuration, in which the two atoms are in same atomic layer (corresponding to the first-neighbor configuration), is not the ground state, with the total energy of ~220 meV higher than the A-type case, even though a weak FM character (~18 meV) was obtained. As a consequence, the calculated AFM coupling strength of Mo is of the order of 30 meV with the ground state typically happening at the second-neighbor configuration. Note also here that for Mo impurity, although the third-neighbor configuration is less stable, the AFM coupling strength is stronger than that of the second-neighbor one. This implies that the Mo can be doped into Bi_2Se_3 (up to the second-neighbor configuration) and also that the A-type AFM is robust with a separation distance of ~6.3 Å and a concentration of ~10%. (See Table II in the Appendix.) The calculated AFM character can be understood in terms of the exchange coupling between the magnetic moments along the antiparallel direction, i.e., the coupling between the nearly fully occupied majority spin states (three p-d hybridized bands of t_{2g} manifold, near the Fermi level) and the unoccupied minority spin states (behaving moderately delocalized high above the Fermi level) will dominate in

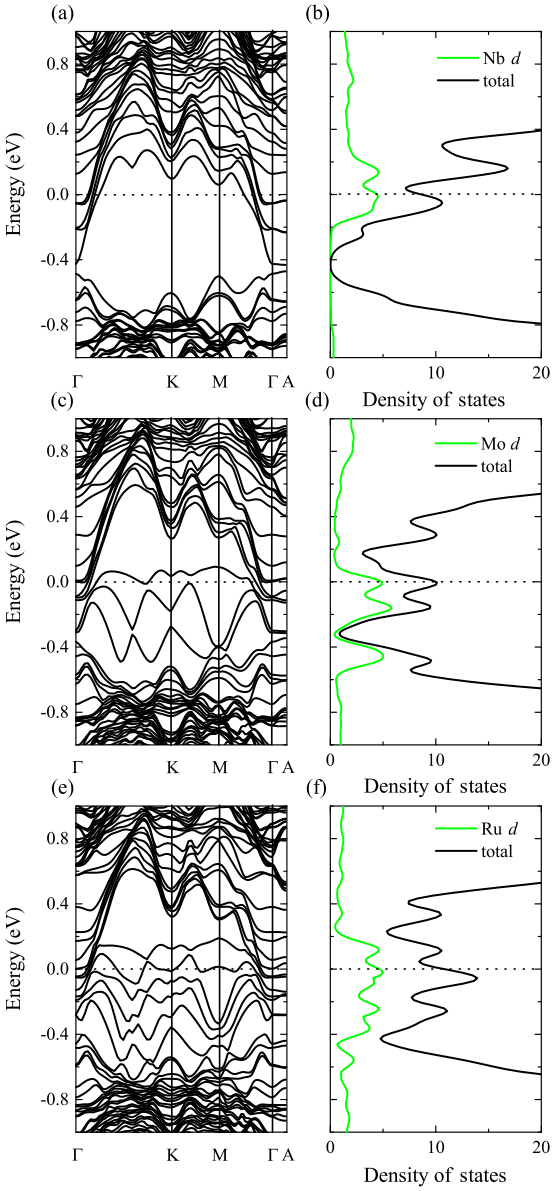

FIG. 1. Calculated band structures and projected density of states for (a), (b) Nb; (c), (d) Mo; and (e), (f) Ru-doped Bi_2Se_3. The Fermi level is set to zero, as indicated by the dotted line. The SOC is taken into account in the calculation.

the magnetic ground states. Also from the calculated band structure in Fig. 1(c), apparently we see that the Mo-doped Bi_2Se_3 has a gapless character, implying a transformation from the insulating to a metallic state upon doping, in the presence of SOC, and hence without a gapped topological state.

Different from Mo, we found that Nb atoms can create a magnetic moment of 1.76 μB, smaller than that of Mo, but with a very strong FM coupling strength. The calculated magnetic coupling strength is of the order of 60 meV with the second-neighbor configuration as the ground state. The coupling strength is six times of magnitude larger than that of Cr ($\sim$10 meV), which has been proven sufficient to achieve QAHE; also comparable to the AFM coupling of Mo, the FM coupling of Nb here remains rather robust at the third-neighbor distance. The strong FM behavior obtained can be understood in terms of the exchange coupling between the partially occupied electronic bands near the Fermi level, which is shown in Fig. 1(a). Thus, it is reasonable to expect that Nb possesses energetically more stable FM ground states associated with a higher Curie temperature and hence may be a potentially better candidate to realize QAHE in Bi_2Se_3.

However, such an expectation is based on the assumption that the Nb atoms can attain a sufficiently high concentration in order to assume a long-range ordered phase and that the magnetically doped system preserves an insulating character of the Bi_2Se_3 host. Unfortunately, the calculated formation energy and the band structure of Nb_{Bi} turned out to be negative on both of these accounts. As shown in Figs. 1(c) and 1(d), although the Nb-doped Bi_2Se_3 system has a band gap of 30 meV, the Fermi level is located at the conduction band, showing an n-type character. Also, the formation energy of Nb is rather high at 1.31 eV, even under the most favorable Bi-rich conditions. It is worth noting that such chemical potential dependence is quite different from the cases for the $3d$ TM or $4f$ TM impurities doped in Bi_2Se_3; as in the latter cases, the formation energy minima always occurs under the Se-rich conditions [18,28]. This is because, to avoid the formation of their competitive second phases (denoted here as TM_xSe_y), the maximum chemical potential of the TM atoms should depend on their chemical potential in the TM_xSe_y. Such dependence is particularly significant for the $4d$ TMs because they form relatively more stable secondary phases in Bi_2Se_3 due to the higher valency of $4d$ TMs in contrast to the $3d$ or $4f$ TMs.

To potentially realize QAHE in Nb-doped Bi_2Se_3, it's essential to be able to reduce the formation energy of Nb_{Bi} while preserving the insulating nature of the TI host. The high formation energy of Nb is largely attributed to its stable secondary phase $NbSe_2$, where Nb has a valency +4 with respect to the valency +3 as being doped in Bi_2Se_3. To suppress the formation of the competitive secondary phase $NbSe_2$, the available chemical potential maximum of Nb is further lowered, leading to relatively high formation energy. In regard to this fact, it is natural to codope some amount of p-type dopant such as group II cations or group V anions with Nb to keep the valency +4 while compensating its n-type conductance character. Here, we considered the substitution of an As atom on Se (As_{Se}) as a typical case since the atomic mass and radius of As are comparable with that of Se. Therefore, the SOC effect and bonding environment should be similar in these two cases.

To strengthen our understanding, we subsequently performed calculations for the acceptor–codoped Nb_{Bi} impurity, regarding the formation energy and the magnetic behavior. The results show that indeed, Nb will undergo a substantial reduction in the formation energy when codoped with an acceptor, i.e., the formation energy of Nb_{Bi} can be lowered to 0.60 eV (by 54%) with the participation of an acceptor impurity. However, at the same time, the magnetic moments are reduced to 0.95 μB, and their FM coupling strength is further lowered to an order of 30 meV but is still sufficiently strong to yield a higher Curie temperature than a Cr impurity can.

To further lower its formation energy, one would expect that a compressive biaxial strain can be beneficial for the Nb incorporation [29] since the ionic radius of Nb is smaller than

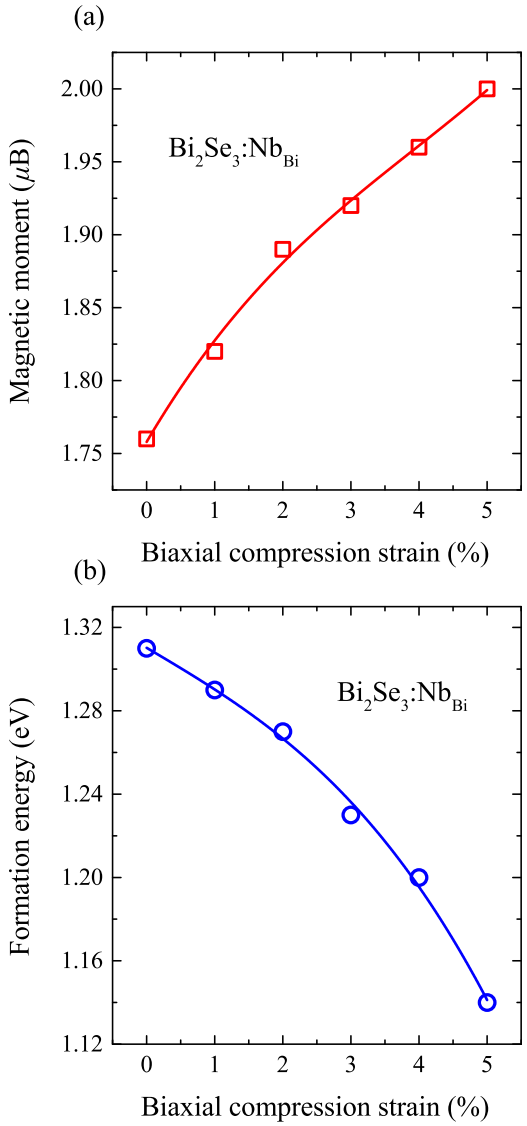

FIG. 2. Calculated (a) magnetic moment and (b) formation energy of the Nb_{Bi} impurity, under biaxial compression strain in the xy plane.

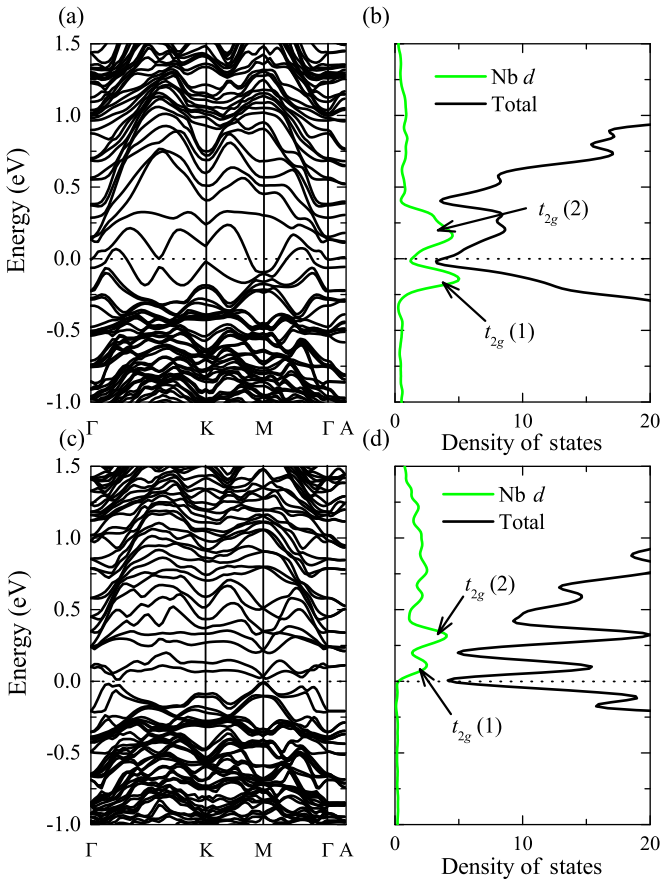

FIG. 3. Calculated band structures and projected density of states for (a), (b) Nb-acceptor pair; (c), (d) Nb-double acceptor complex. The Fermi level is set to zero, as indicated by the dotted line. The SOC is taken into account in the calculation. The fully occupied p states of As acceptor(s) are deep below E_F and not shown in this scheme.

that of Bi^{3+}. In this regard, our calculation has confirmed that the formation energy of Nb_{Bi} can be reduced by 13% upon a 5% compression biaxial strain, while the magnetic moment of Nb_{Bi} can be increased by 14%; as shown in Figs. 2(a) and 2(b), both these two properties show an approximately linear dependence on the strain. This can be understood as the fact that a compressive strain lowers the local inward stress induced by the Nb_{Bi}, making the Nb atoms match the Bi_2Se_3 lattice better with a stabilized geometric configuration, which ensures lower formation energy [29]. Furthermore, the compressive strain also reduces the relative inward distortions around the substitution Nb atoms in Bi_2Se_3, which can play a role in the crystal-field-symmetry protection and, in turn, stabilize the electronic spins; this explains why the magnetic moment is also improved by the compressive strain.

Previous theoretical efforts [28] on the magnetic codoping in the TI system showed that the magnetic moment of the ions can be enhanced by codoping with the donors, which is different from the acceptor codoped case here. This is because the electronic donors will contribute additional occupied states to the majority spins, whereas the codoping acceptors herein lead to additional unoccupied states to the majority spins and therefore lower the total spins and the magnetic moment. Nevertheless, both approaches will lead to reduction of the magnetic coupling strength by compensating the electronic carriers. However, unfortunately, codoping the Nb_{Bi} impurity with one acceptor is unable to create an insulating FM state in the Bi_2Se_3 system, as shown in Fig. 3(a). Although the Fermi level shifts down to a position corresponding to the original gap of Bi_2Se_3, the impurity states are localized around the Fermi level and, in turn, lead to a semimetal phase.

The reason that the Nb_{Bi}-acceptor pair fails to create an insulating magnetic state in Bi_2Se_3 can be understood as a consequence of the reduced correlation in t_{2g} states of Nb: the $4d$ states of Nb exhibit splitting under the approximate octahedron (O_h) symmetry in the Bi_2Se_3 lattice, leading to higher lying, fully symmetric e_g states and lower lying, triply degenerated t_{2g} states. According to the electronic occupation, the e_g states should be situated higher above the conduction band maximum (CBM), leaving behind with the t_{2g} states in/below the bandgap, as can be seen from Fig. 3(b). Upon

the codoping, as the Fermi level shifts down, one of the electrons in the highest occupied t_{2g} state transfers to the acceptor state, whereas the resultant t_{2g} state still coupled strongly with the remaining occupied t_{2g} state below via the p-d hybridization with the p states of Se, dilutes the electron correlation effect. As a consequence, the two t_{2g} band edge states cannot be fully separated in energy to open a finite gap, even with the SOC. On the basis of the above analysis, one would expect that codoping the Nb-acceptor pair with an additional acceptor will avoid this problem and create a gap. To verify this expectation, we have performed calculations on such a configuration. Indeed, as the remaining one electron is removed from the t_{2g} state, the resultant t_{2g} band turns to be fully unoccupied and shifts up to a higher energy, yielding a tiny gap (about 10 meV) around the Fermi level as shown in Fig. 3(c), owing to the fact that the interaction between the unoccupied t_{2g} band and the host valence band maximum (VBM) is not that strong. Such a configuration, however, is still not applicable to QAHE. Because the 4d orbitals of an Nb impurity are fully unoccupied [see Fig. 3(d)] at the same time, the system turns to be nonmagnetic with the long-range magnetic coupling gone.

Therefore, in addition to the previously proposed codoping approach [13,28] in realizing an insulating FM state in the Be_2Se_3 family, one should also pay attention to the impurity band edge coupling effect, in particular the reduced correlation in t_{2g} states of d metals. A most straightforward model to test this rule is the Cr-doped $(Bi_xSb_{1-x})_2Te_3$, in which the Cr atom ($3d^54s^1$) has a valency of +3 and also three electrons occupying the 3d orbitals. Therefore, there is no such band edge coupling problem, and the occupied t_{2g} band can be naturally gapped with the unoccupied e_g states due to their symmetry distinction, with the latter located in the conduction band. Besides, additional examples should be V-donor codoped $(Bi_xSb_{1-x})_2Te_3$ and Eu-donor codoped Bi_2Se_3, where the introduced codopants could act as electron providers, which can donate electrons to the nonisovalent magnetic impurity and make the triplet t_{2g} states or f states fully occupied, whereby the band edge coupling problem is also avoided. The above mentioned systems have all proven successful in realizing insulating ferromagnetism [1,13,28] for QAHE application, experimentally and/or theoretically. However, due to the lower electronegativity of Nb, the t_{2g} states are partially localized in the gap and, hence, to make such an impurity state fully occupied, will not help to achieve the insulating phase. On the other hand, one cannot make the t_{2g} states of Nb fully occupied even by electron doping (the t_{2g} states of Nb are partially overlapped with the CBM and thus the as-doped electrons should be delocalized in the CB, behaving as free carries). Therefore, one needs to compensate the impurity-induced *gap states* by electron acceptors, which is what we have described in this paper, whereas the gap opening will be further prevented herein by the band edge coupling in terms of the reduced correlation in t_{2g} manifold. This rationale provides insight into why this 4d TM cannot be doped for QAHE in the Bi_2Se_3 family. The whole analysis also suggests that although the nonisovalent magnetic impurity-induced carrier can be compensated and whereby the dopability of the system can also be improved, the initial gap of the magnetically doped TI (herein 30 meV for Nb-doped Bi_2Se_3) may not be preserved upon codoping (e.g., single acceptor and Nb codoped Bi_2Se_3) due to d band (or f band) edge coupling. Generally, the multivalency nature of TMs with stable secondary phases can be a major challenge to realizing QAHE.

IV. CONCLUSIONS

In conclusion, in this paper we probed the electronic and magnetic properties of 4d TM-doped Bi_2Se_3. We discovered among the 4d TM impurities that Mo may be a potential candidate for topological superconducting application in Bi_2Se_3 as it possesses a relatively large magnetic moment with a strong AFM character being predicted. Besides, although having a stable FM character with improved thermodynamic stability upon codoping or compressive misfit strain, Nb impurity is still unable to support the QAH state in Bi_2Se_3 mainly due to the reduced correlation in t_{2g} states. This rationale is not only found to be universal in explaining why such TMs cannot create a QAH state in the Bi_2Se_3 system but is also particularly important to fully understand the principle of acquisition of insulating FM states inside TI and, thus, may behave as a guideline for the relevant experimental framework. Our results and findings may have important implications for the Bi_2Se_3 types of materials in topological superconducting and QAHE applications.

ACKNOWLEDGMENTS

This paper is supported by the Early Career Scheme grant from University Grants Committee of Hong Kong (Grant No. 24300814) and a direct grant from the Chinese University of Hong Kong (Grant No. 4053084).

APPENDIX: MAGNETIC COUPLING STRENGTHS OF Nb AND Mo IMPURITY WITH DIFFERENT DISTANCES AND SPIN CONFIGURATIONS

The energies and FM/AFM coupling strengths of Nb/Mo doped Bi_2Se_3 with different configurations were calculated, as listed in Table II, which enables us to conclude that the Nb impurity favors an FM ground state with a coupling strength of 69.5 meV, and Mo favors an AFM ground state with a coupling strength of 32 meV.

TABLE II. Relative energies (in meV) and FM/AFM coupling strengths ($\Delta E_{\mathrm{FM-AFM}}/2$, in meV) of Nb and Mo in different configurations. The relative energy is defined as the energy difference between a given configuration and the most stable (ground states) configuration.

	Nb_{FM}	Nb_{AFM}	$\Delta E_{\mathrm{FM-AFM}}/2$	Mo_{FM}	Mo_{AFM}	$\Delta E_{\mathrm{FM-AFM}}/2$
First neighbor (same layer)	188	417	− 114.5	220	256	−18
Second neighbor (different layers)	0	139	− 69.5	64	0	32
Third neighbor (different layers)	251	550	− 149.5	690	435	127.5

[1] C.-Z. Chang, J. Zhang, X. Feng, J. Shen, Z. Zhang, M. Guo, K. Li, Y. Ou, P. Wei, L.-L. Wang, Z.-Q. Ji, Y. Feng, S. Ji, X. Chen, J. Jia, X. Dai, Z. Fang, S.-C. Zhang, K. He, Y. Wang *et al.*, Science **340**, 167 (2013).

[2] C.-Z. Chang, W. Zhao, D. Y. Kim, H. Zhang, B. A. Assaf, D. Heiman, S.-C. Zhang, C. Liu, M. H. W. Chan, and J. S. Moodera, Nat. Mater. **14**, 473 (2015).

[3] J. G. Checkelsky, R. Yoshimi, A. Tsukazaki, K. S. Takahashi, Y. Kozuka, J. Falson, M. Kawasaki, and Y. Tokura, Nat. Phys. **10**, 731 (2014).

[4] X. Kou, S.-T. Guo, Y. Fan, L. Pan, M. Lang, Y. Jiang, Q. Shao, T. Nie, K. Murata, J. Tang, Y. Wang, L. He, T.-K. Lee, W.-L. Lee, and K. L. Wang, Phys. Rev. Lett. **113**, 137201 (2014).

[5] A. Kandala, A. Richardella, S. Kempinger, C.-X. Liu, and N. Samarth, Nat. Commun. **6**, 7434 (2015).

[6] X. Kou, L. Pan, J. Wang, Y. Fan, E. S. Choi, W.-L. Lee, T. Nie, K. Murata, Q. Shao, S.-C. Zhang, and K. L. Wang, Nat. Commun. **6**, 8474 (2015).

[7] Y. Feng, X. Feng, Y. Ou, J. Wang, C. Liu, L. Zhang, D. Zhao, G. Jiang, S.-C. Zhang, K. He, X. Ma, Q.-K. Xue, and Y. Wang, Phys. Rev. Lett. **115**, 126801 (2015).

[8] M. Mogi, R. Yoshimi, A. Tsukazaki, K. Yasuda, Y. Kozuka, K. S. Takahashi, M. Kawasaki, and Y. Tokura, Appl. Phys. Lett. **107**, 182401 (2015).

[9] X. Zhang and S.-C. Zhang, Proc. SPIE Int. Soc. Opt. Eng. **8373**, 837309 (2012).

[10] X.-L. Qi and S.-C. Zhang, Rev. Mod. Phys. **83**, 1057 (2011).

[11] G. Xu, J. Wang, C. Felser, X.-L. Qi, and S.-C. Zhang, Nano Lett. **15**, 2019 (2015).

[12] J. Hu, Z. Zhu, and R. Wu, Nano Lett. **15**, 2074 (2015).

[13] S. Qi, Z. Qiao, X. Deng, E. D. Cubuk, H. Chen, W. Zhu, E. Kaxiras, S. B. Zhang, X. Xu, and Z. Zhang, Phys. Rev. Lett. **117**, 056804 (2016).

[14] H. P. Wang, W. Luo, and H. J. Xiang, Phys. Rev. B **95**, 125430 (2017).

[15] Z. F. Wang, Z. Liu, and F. Liu, Phys. Rev. Lett. **110**, 196801 (2013).

[16] X. F. Kou, W. J. Jiang, M. R. Lang, F. X. Xiu, L. He, Y. Wang, Y. Wang, X. X. Yu, A. V. Fedorov, P. Zhang, and K. L. Wang, J. Appl. Phys. **112**, 063912 (2012).

[17] Y. Ni, Z. Zhang, I. C. Nlebedim, R. L. Hadimani, G. Tuttle, and D. C. Jiles, J. Appl. Phys. **117**, 17C748 (2015),

[18] J. M. Zhang, W. Zhu, Y. Zhang, D. Xiao, and Y. Yao, Phys. Rev. Lett. **109**, 266405 (2012).

[19] R. Yu, W. Zhang, H.-J. Zhang, S.-C. Zhang, X. Dai, and Z. Fang, Science **329**, 61 (2010).

[20] G. Kresse and J. Furthmuller, Phys. Rev. B **54**, 11169 (1996).

[21] J. P. Perdew, K. Burke, and M. Ernzerhof, Phys. Rev. Lett. **77**, 3865 (1996).

[22] G. Kresse and D. Joubert, Phys. Rev. B **59**, 1758 (1999).

[23] C. G. Van de Walle and J. Neugebauer, J. Appl. Phys. **95**, 3851 (2004).

[24] J.-M. Zhang, W. M. Ming, Z. G. Huang, G.-B. Liu, X. F. Kou, Y. B. Fan, K. L. Wang, and Y. G. Yao, Phys. Rev. B **88**, 235131 (2013).

[25] M. Miyamoto, H. Mukuda, T. Kobayashi, M. Yashima, Y. Kitaoka, S. Miyasaka, and S. Tajima, Phys. Rev. B **92**, 125154 (2015).

[26] A. T. Romer, I. Eremin, P. J. Hirschfeld, and B. M. Andersen, Phys. Rev. B **93**, 174519 (2016).

[27] M. P. Allan, K. Lee, A. W. Rost, M. H. Fischer, F. Massee, K. Kihou, C-H. Lee, A. Iyo, H. Eisaki, T-M. Chuang, J. C. Davis, and E.-A. Kim, Nat. Phys. **11**, 177 (2015).

[28] B. Deng, Y. O. Zhang, S. B. Zhang, Y. Y. Wang, K. He, and J. Y. Zhu, Phys. Rev. B **94**, 054113 (2016).

[29] J. Y. Zhu, F. Liu, G. B. Stringfellow, and S.-H. Wei, Phys. Rev. Lett. **105**, 195503 (2010).